THE JOURNAL OF BIOLOGICAL CHEMISTRY
Vol. 280, No. 13, Issue of April 1, pp. 13153–13162, 2005
Printed in U.S.A.

mRNA Guanylation Catalyzed by the *S*-Adenosylmethionine-dependent Guanylyltransferase of Bamboo Mosaic Virus*

Received for publication, November 8, 2004, and in revised form, January 24, 2005
Published, JBC Papers in Press, January 25, 2005, DOI 10.1074/jbc.M412619200

Yih-Leh Huang‡, Yau-Heiu Hsu, Yu-Tsung Han, and Menghsiao Meng§

From the Graduate Institute of Biotechnology, National Chung Hsing University, 250 Kuo-Kuang Rd., Taichung, Taiwan 40227, Republic of China

The *S*-adenosylmethionine-dependent guanylyltransferase of bamboo mosaic virus belongs to a novel class of mRNA capping enzymes distantly conserved in *Alphavirus*-like superfamily. The reaction sequence of the viral enzyme has been proposed comprising steps of 1) binding of GTP and *S*-adenosylmethionine, 2) formation of m^7GTP and *S*-adenosylhomocysteine, 3) formation of the covalent (Enzyme-m^7GMP) intermediate, and 4) transfer of m^7GMP from the intermediate to the RNA acceptor. In this study the acceptor specificity of the viral enzyme was characterized. The results show that adenylate or guanylate with 5′-diphosphate group is an essential feature for acceptors, which can be RNA or mononucleotide, to receive m^7GMP. The transfer rate of m^7GMP to guanylate is greater than to adenylate by a factor of ~3, and the K_m value for mononucleotide acceptor is ~10^3-fold higher than that for RNA. The capping efficiency of the viral genomic RNA transcript depends on the length of the transcript and the formation of a putative stem-loop structure, suggesting that mRNA capping process may participate in regulating the viral gene expression.

The 5′ cap structure, m^7G(5′)ppp(5′)N, of mRNA serves as a recognition site for ribosome binding in translation and is important for the stability of mRNA against the attack of 5′ exonuclease in eukaryotic cells. A series of three nuclear enzymatic activities is responsible for the formation of the cap structure (1). First, the γ-phosphate at the 5′ end of nascent mRNA is removed by RNA 5′-triphosphatase; second, the GMP moiety of GTP molecule is transferred to the 5′-diphosphate end of the RNA via a 5′-5′ linkage by guanylyltransferase; and finally, a methyl group is added to N7 of the transferred guanylate from *S*-adenosylmethionine (AdoMet)[1] by methyltransferase. The cap formation pathway for viruses within the *Alphavirus*-like superfamily differs from the nuclear mechanism in that methylation of GTP occurs before transguanylation; in other words, m^7GMP, rather than GMP, is transferred to the 5′ end of the 5′-diphosphate RNA during the cap formation process. This distinctive mRNA capping reaction is catalyzed by a group of distantly conserved AdoMet-dependent guanylyltransferases that were identified in Semliki Forest virus (2), hepatitis E virus (3), tobacco mosaic virus (4), brome mosaic virus (5, 6), and bamboo mosaic virus (BaMV) (7). Together with other characteristics such as their membrane-association nature and distinctive protein primary structures, this class of enzyme represents a novel mRNA capping enzyme different from those evolutionally conserved guanylyltransferases and methyltransferases in DNA viruses, metazoans, and fungi. Although the critical roles of the conserved amino acids in the enzymatic activities of the enzyme of Semliki Forest virus (8) and BaMV (9) have been addressed, the molecular mechanism of this class of enzyme is far from being understood.

BaMV, a member of *Alphavirus*-like superfamily, has a ~6.4- kilobase positive-strand RNA genome with a cap structure at the 5′ end and a poly(A) tail at the 3′ end (10). Open reading frame 1 of the viral genome encodes a 155-kDa replicase consisting of three functional domains. The N-terminal 442 amino acids constitute a mRNA capping enzyme domain exhibiting an AdoMet-dependent guanylyltransferase activity (7), the central region is a helicase-like domain harboring NTPase and RNA 5′-triphosphatase activities (11), and the C-terminal part of the viral protein is an RNA-dependent RNA polymerase domain (12) that binds specifically to the 3′-pseudoknot structure of the viral RNA genome *in vitro* (13). Two subgenomic RNAs with lengths of ~2 and ~1 kilobases are produced during the replication cycle of the virus. The former subgenomic RNA encodes proteins required for the viral movement, whereas the latter is responsible for the production of the viral coat protein. A simple working model for the BaMV capping enzyme consisting of four reaction steps has been proposed based mainly on results of site-directed mutagenesis (9). 1) GTP and AdoMet bind to the enzyme at close proximity to each other. 2) The methyl group from AdoMet is transferred to GTP, leading to the generation of m^7GTP and AdoHcy. 3) An unidentified amino acid links covalently to the m^7GMP moiety of m^7GTP via a phosphoamide bond, resulting in the formation of the covalent [Enzyme-m^7GMP] intermediate. Persistent binding of AdoHcy to the enzyme is required for the formation of the covalent intermediate. 4) The m^7GMP of the covalent intermediate is then transferred to the 5′ end of nascent RNA, whose 5′ γ-phosphate has been removed by RNA 5′-triphosphatase activity localized to the helicase-like domain of the viral replicase to form the 5′ cap structure. The apparent activity of AdoMet-dependent guanylyltransferase can, thus, be divided into GTP methyltransferase and m^7GTP:mRNA guanylyltransferase activities as shown below. For GTP methyltransferase, enzyme + GTP + AdoMet → enzyme + m^7GTP + AdoHcy (steps 1 and 2). For m^7GTP:mRNA guanylyltransferase, enzyme + m^7GTP + AdoHcy → [Enzyme-m^7GMP] + PPi + AdoHcy (step 3) and [Enzyme-m^7GMP] + ppRNA → m^7GMP-ppRNA + enzyme step (Step 4).

* This study was supported by National Science Council, Taiwan, Republic of China Grants NSC 92-2313-B-005-071 and NSC 93-2313-B-005-052. The costs of publication of this article were defrayed in part by the payment of page charges. This article must therefore be hereby marked "*advertisement*" in accordance with 18 U.S.C. Section 1734 solely to indicate this fact.

‡ Present address: Institute of Molecular Biology, Academia Sinica, Nankang, Taipei, Taiwan 11529, Republic of China.

§ To whom correspondence should be addressed. Tel.: 886-4-22840328; Fax: 886-4-22853527; E-mail: mhmeng@dragon.nchu.edu.tw.

[1] The abbreviations used are: AdoMet, *S*-adenosylmethionine; BaMV, bamboo mosaic virus; AdoHcy, adenosylhomocysteine; pp, pyrophosphate.

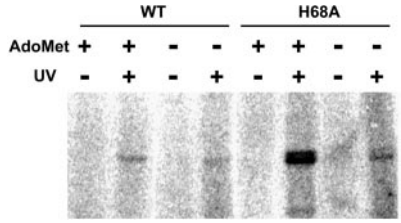

FIG. 1. **Effect of AdoMet on GTP cross-linking.** Cross-linking of GTP to the BaMV capping enzyme was assayed by irradiating the reaction mixture that contained the purified enzyme and [γ-^{32}P]GTP with UV light in conditions described under "Experimental Procedures." The UV-cross-linked products were analyzed by SDS-PAGE (10%). To prevent the formation of the ^{32}P-labeled covalent [Enzyme-m^{7}GMP] intermediate, [γ-^{32}P]GTP and EDTA were used in the reaction mixture. *WT*, wild type.

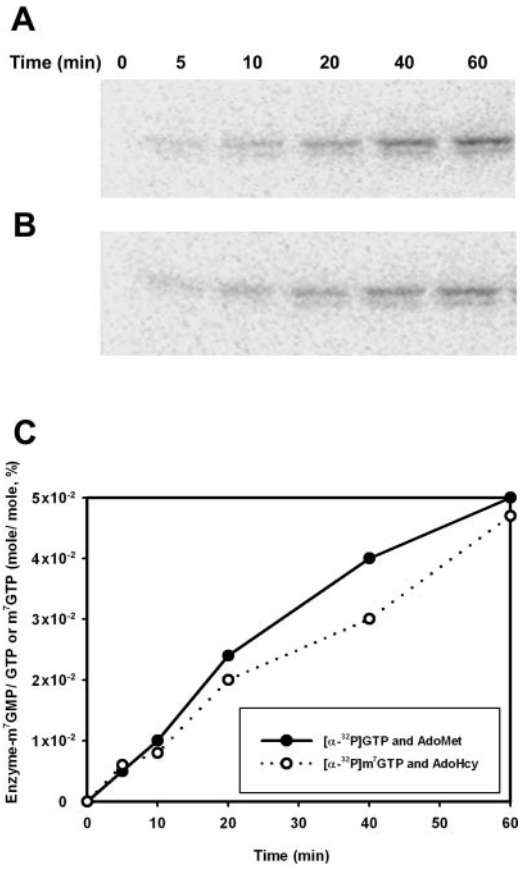

FIG. 2. **The relative rates of formation of the covalent [Enzyme-m^{7}GMP] intermediate by reactions started with [α-^{32}P]GTP and AdoMet or with [α-^{32}P]m^{7}GTP and AdoHcy.** Reactions were carried out at 30 °C for the indicated times in conditions as described under "Experimental Procedures." [α-^{32}P]GTP and [α-^{32}P]m^{7}GTP in same concentration and specific radioactivity were used. *Panel A*, a phosphorimage showing the accumulation of the covalent intermediate with the incubation time by reactions started with [α-^{32}P]GTP and AdoMet. *Panel B*, same as *panel A*, except reactions were started with [α-^{32}P]m^{7}GTP and AdoHcy. *Panel C*, time courses of the molar yield of the covalent intermediate under reaction conditions of *panel A* and *B*.

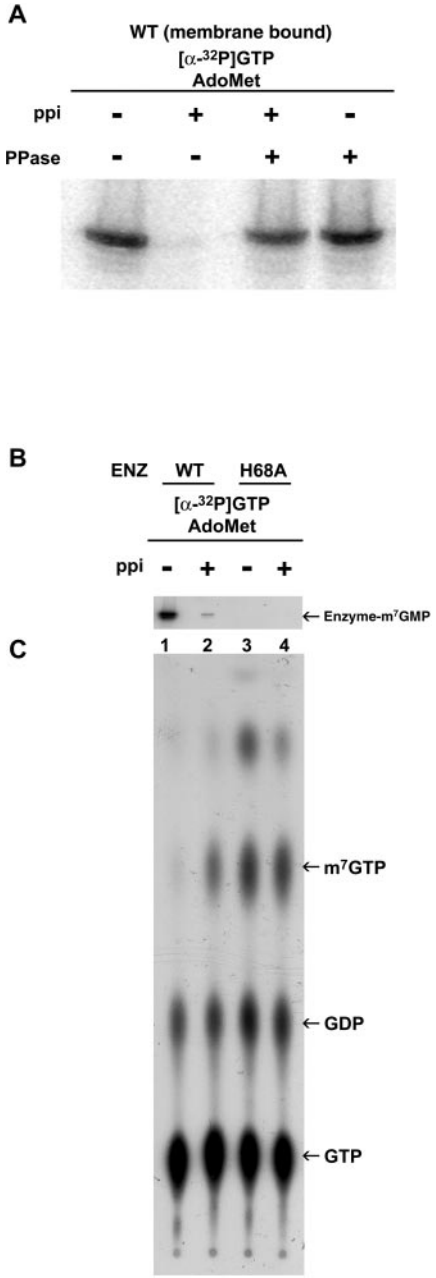

FIG. 3. **Pyrophosphate effects on the formation of the covalent [Enzyme-m^{7}GMP] intermediate.** *Panel A*, the BaMV capping enzyme in the yeast membrane preparation was incubated with [α-^{32}P]GTP and AdoMet in conditions as described under "Experimental Procedures." Pyrophosphate (1 mM) and pyrophosphatase (1 unit) were included at different combinations as indicated in the reactions. The covalent intermediate was visualized by phosphorimaging after the reaction products were separated by SDS-PAGE (10%). *WT*, wild type. *Panels B* and *C*, the purified wild type or H68A mutant enzyme (*ENZ*) was incubated with [α-^{32}P]GTP and AdoMet in reaction conditions as described under "Experimental Procedures." Pyrophosphate (1 mM) was included in some reactions as indicated. When reactions were over, half of the products was analyzed by SDS-PAGE (10%) and visualized by phosphorimaging to detect the covalent [Enzyme-m^{7}GMP] intermediate (*panel B*), and the second half was subjected to TLC analysis as described under "Experimental Procedures" (*panel C*). *Arrows* indicate the migration positions of standards (m^{7}GTP, GDP, and GTP) on the TLC plate.

The two-activity-coupling notion in the context of the proposed model was supported by a couple of lines of evidence. 1) Substitution of His-68 by Ala in the BaMV capping enzyme increased the GTP methyltransferase activity but disabled the enzyme from forming the covalent [Enzyme-m^{7}GMP] intermediate (9); 2) the wild-type capping enzyme could form the covalent intermediate in the presence of m^{7}GTP and AdoHcy. To provide more details regarding each of the steps in the proposed model and for better understanding of the replication mechanism of BaMV, the viral capping enzyme and the covalent [Enzyme-m^{7}GMP] intermediate were purified and characterized in this study. The step of transferring m^{7}GMP from the covalent intermediate to RNA acceptor was particularly addressed.

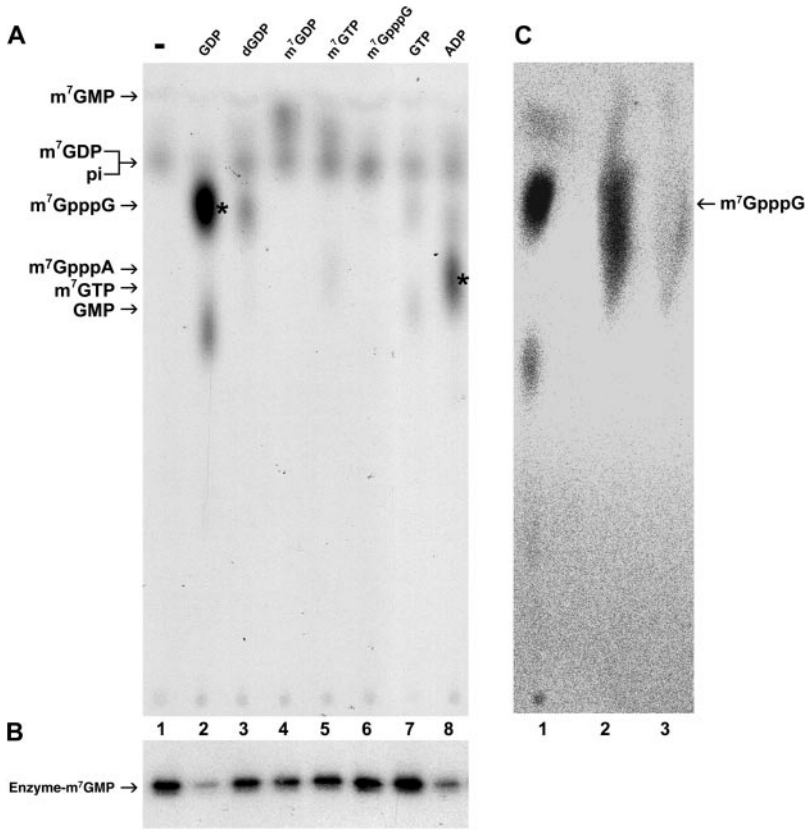

FIG. 4. **Formation of m^7GpppG and m^7GpppA.** *Panels A* and *B*, a variety of nucleotides (each 1 mM) were incubated individually with the ^{32}P-labeled covalent [Enzyme-m^7GMP] intermediate at 30 °C for 2 h in buffer conditions as described under "Experimental Procedures." Half of the reaction mixture was then subjected to TLC analysis (*panel A*). *Arrows along* the *edge* of the TLC plate indicate the migration positions of standards. *Asterisks* mark the spots of m^7GpppG and m^7GpppA. The other half of the reaction mixture was subjected to SDS-PAGE analysis to determine the residual covalent intermediate after reactions (*panel B*). *Lane 1* is a control without adding nucleotides in the reaction. *Panel C*, the two products appearing on *lane 2*, *panel A*, were extracted by 1 M ammonium acetate buffer (pH 6.7) and treated separately with nuclease P1 at 37 °C for 1 h. The nuclease-digested products were then analyzed by TLC. *Lane 1*, the extracts before nuclease P1 treatment; *lane 2*, the digested product from the spot marked with an *asterisk* on *lane 2*, *panel A*; *lane 3*, the product from the slowly migrating spot shown on *lane 2*, *panel A*.

EXPERIMENTAL PROCEDURES

Chemicals—General chemicals and nucleotides (including m^7GTP and m^7GDP) were purchased from Sigma, whereas AdoMet, m^7GpppG, and m^7GpppA were from New England BioLabs. [α-^{32}P]GTP (3000 Ci/mmol) and [γ-^{32}P]GTP (3000 Ci/mmol) were obtained from PerkinElmer Life Sciences, and [α-^{32}P]m^7GTP was synthesized in this study by the H68A mutant in reactions with [α-^{32}P]GTP and AdoMet and purified with high performance liquid chromatography as described previously (9).

Protein Purification—The BaMV capping enzyme, fused with a His tag at its C terminus, was expressed in *Saccharomyces cerevisiae* and purified by a protocol consisting of steps of membrane fractionation, detergent extraction, and metal affinity chromatography as described previously (9). The enzyme finally was in 50 mM Tris-HCl (pH 8.0) buffer with 150 mM NaCl, 5 mM β-mercaptoethanol, 10% glycerol, and 0.3% Sarkosyl. The ^{32}P-labeled covalent [Enzyme-m^7GMP] intermediate was purified with a 3 ml of nickel nitrilotriacetic acid chromatography column (Qiagen) from a reaction mixture of 100 μg of the purified capping enzyme, 0.015 μM [α-^{32}P]GTP, and 0.5 mM AdoMet in a 2-ml reaction buffer (50 mM Tris-HCl (pH 8.0), 75 mM NaCl, 5 mM KCl, 1 mM $MgCl_2$, 2.5 mM β-mercaptoethanol, 2.5 mM dithiothreitol, 5% glycerol, 0.15% Sarkosyl, and 0.6% *n*-octyl-β-D-glucopyranoside). The purification protocol consisted of a washing step with 300 ml of reaction buffer and an elution step with 10 ml of elution buffer that contained 500 mM imidazole. The purified covalent intermediate was finally dialyzed in the same buffer as that preserved the purified BaMV capping enzyme. The helicase-like domain of the BaMV replicase was purified as described previously (11).

RNA Preparation—The RNA molecule with a 5′ guanylate followed by 25 consecutive cytidylates, designated as $G(C)_{25}$, was synthesized *in vitro* by using T7-MEGAshortscript kit (Ambion) with a double-strand DNA template annealed from oligonucleotides 5′-AATTTAATACGACTCACTATA**G**$(C)_{25}$ and 5′-$(G)_{25}$**C**TATAGTGAGTCGTATTAAAATT. The underlined sequence represents the classic T7 promoter. CTP and GTP, GDP, or GMP (each 7.5 mM) were included in the reactions to synthesize $pppG(C)_{25}$, $ppG(C)_{25}$, or $pG(C)_{25}$, respectively. $A(C)_{25}$ was synthesized similarly with a template annealed from oligonucleotides 5′-AATTTAATACGACTCACTATT**A**$(C)_{25}$ and 5′-$(G)_{25}$**T**AATAGTGAGTCGTATTAAAATT. The underlined sequence represents a class II T7 promoter that allows transcription to start from adenylate (14). CTP and ATP, ADP, or AMP (each 7.5 mM) were used to synthesize $pppA(C)_{25}$, $ppA(C)_{25}$, or $pA(C)_{25}$, respectively. RNA molecules related to the BaMV sequence were also synthesized *in vitro* with cDNA templates composed of the classic T7 promoter and corresponding regions of the BaMV genome. [γ-^{32}P]GTP was included in the *in vitro* transcription reactions when 5′-[γ-^{32}P]RNA was synthesized. All RNA molecules were finally purified by 8 M urea, PAGE. To remove the 5′ γ-phosphate of the BaMV RNA, 0.2 μM concentrations of the respective 5′-[γ-^{32}P]RNA was incubated with 100 ng of the helicase-like domain of the BaMV replicase in a buffer that also contained 3 mM Tris-HCl (pH 8.0), 15 mM KCl, 10 mM dithiothreitol, and 10 units of RNase inhibitor at 20 °C for 2 h.

GTP Cross-linking—Ten μl of the purified capping enzyme (0.1 μg) was mixed with 10 μl of solution that contained 0.15 μM [γ-^{32}P]GTP, 50 mM Tris-HCl (pH 8.0), 5 mM dithiothreitol, 10 mM KCl, 5 mM EDTA, and 1.2% *n*-octyl-β-D-glucopyranoside and then placed into a 96-well plate in the presence or absence of 1 mM AdoMet. The mixture was irradiated on ice by using a single 15-W germicidal UV lamp held at a distance of 10 cm for 30 min. After adding with SDS (final 2%), the UV-cross-linked products were analyzed by SDS-PAGE (10%) and visualized by phosphorimaging.

Formation of the Covalent [Enzyme-m^7GMP] Intermediate—To determine the relative rates of forming the covalent intermediate using different nucleotide substrates, the purified capping enzyme (0.1 μg) was incubated with [α-^{32}P]GTP (0.015 μM) and AdoMet (100 μM) or with [α-^{32}P]m^7GTP (0.015 μM) and AdoHcy (100 μM) at 30 °C for various times in a final 20-μl reaction buffer. To determine the pyrophosphate effect, the purified capping enzyme (0.1 μg), [α-^{32}P]GTP (0.15 μM), AdoMet (0.5 mM), and pyrophosphate (1 mM) were included in a 20-μl reaction buffer at 30 °C for 90 min. When reactions involved inorganic pyrophosphatase, the partially purified capping enzyme (total 10 μg), still associated with yeast membrane fraction, was used in the reaction buffer without the addition of Sarkosyl. SDS (final 2%) was added at the ends of reactions, and formation of the ^{32}P-labeled covalent intermediate was analyzed by SDS-PAGE (10%) and visualized by phosphorimaging.

Transfer of m^7GMP from the Covalent [Enzyme-m^7GMP] Intermediate to Acceptors—Various nucleotides and RNA molecules were tested as acceptors in this study. The acceptor, at the concentrations indicated in figure legends 4–10, was incubated with the ^{32}P-labeled covalent intermediate in a 20-μl reaction buffer. The reaction was carried out at 30 °C for indicated periods of time. When the reactions were over, half of the reaction mixture was subjected to SDS-PAGE (10%) analysis, and

the other half was subjected to TLC analysis.

TLC—The enzyme reaction solution was extracted repeatedly with phenol/chloroform and chloroform, and the products in aqueous phase were analyzed by spotting 1 μl of the sample onto a polyethyleneimine-cellulose TLC plate (20 × 20 cm) that was later developed with 0.45 M $(NH_4)_2SO_4$ and visualized by phosphorimaging. The migration positions of standards were observed under UV light.

RESULTS

GTP Binding—A previous mutational study showed that the presence of AdoHcy is essential for the BaMV capping enzyme to react with m^{7}GTP and form the covalent [Enzyme-m^{7}GMP] intermediate (9). A crucial change of protein conformation induced by AdoHcy binding may involve this event. Because AdoMet and AdoHcy are structurally related, it became interesting to know whether AdoMet has a role in assisting the binding of GTP by inducing a similar protein conformational change. In this study, the binding affinity of the BaMV capping enzyme for GTP was assayed indirectly by irradiating the reaction mixture of the enzyme with [γ-^{32}P]GTP in the presence or absence of AdoMet using a UV lamp (Fig. 1). Because [γ-^{32}P]GTP, rather than [α-^{32}P]GTP, was used in the reaction and EDTA was added to prevent the formation of the covalent [Enzyme-m^{7}GMP] intermediate, the protein bands appearing with radioactivity on the gels of SDS-PAGE should be the UV-cross-linked products. The data clearly showed that AdoMet could enhance both the wild type and H68A mutant to cross-link to GTP, suggesting that either the affinity for GTP was enhanced or the protein conformation was altered so that a photoreactive moiety was brought closer to GTP. The stronger cross-linking to GTP observed in H68A is consistent with the greater GTP methyltransferase activity of the mutant enzyme.

The Rate-determining Step in the Path toward Forming the Covalent [Enzyme-m^{7}GMP] Intermediate—The covalent intermediate could be formed through reactions initiated with either GTP and AdoMet or m^{7}GTP and AdoHcy (9). Conceivably, the catalytic steps involved in the former reaction include a methyl transfer from AdoMet to GTP and the subsequent m^{7}GMP transfer from m^{7}GTP to the enzyme. In contrast, the latter reaction involves only the transfer of m^{7}GMP. The relative formation rates of the covalent intermediate through the two reaction conditions were determined (Fig. 2). The nearly identical rates suggest that the methyl transfer from AdoMet to GTP occurs at a much greater rate than the transfer of m^{7}GMP from m^{7}GTP to the enzyme at the reaction conditions; in other words, the transfer of m^{7}GMP is likely the rate-determining step along the course from the original substrates, GTP and AdoMet, to the covalent [Enzyme-m^{7}GMP] intermediate.

Pyrophosphate Effect—To know whether pyrophosphate exerts a feedback inhibition against the formation of the covalent [Enzyme-m^{7}GMP] intermediate, it was included in the reaction mixture containing the BaMV capping enzyme, [α-^{32}P]GTP, and AdoMet. The results showed that pyrophosphate indeed exhibited an inhibitory effect on the formation of the covalent intermediate, and this effect could be counteracted by pyrophosphatase (Fig. 3*A*). Besides inhibiting the formation of the covalent intermediate, pyrophosphate simultaneously increased the accumulation of m^{7}GTP in the reaction solution of the wild-type enzyme (Fig. 3, *B* and *C*, *lanes 1* and *2*). As expected, H68A did not response to pyrophosphate (Fig. 3, *B* and C, *lanes 3* and *4*) because it already lost the ability to form the covalent intermediate. The results also suggested that pyrophosphate has no effect on GTP methylation. Again, the results agree with the proposed reaction sequence of the BaMV capping enzyme in which blocking the step of forming the covalent intermediate would definitely result in the accumulation of m^{7}GTP.

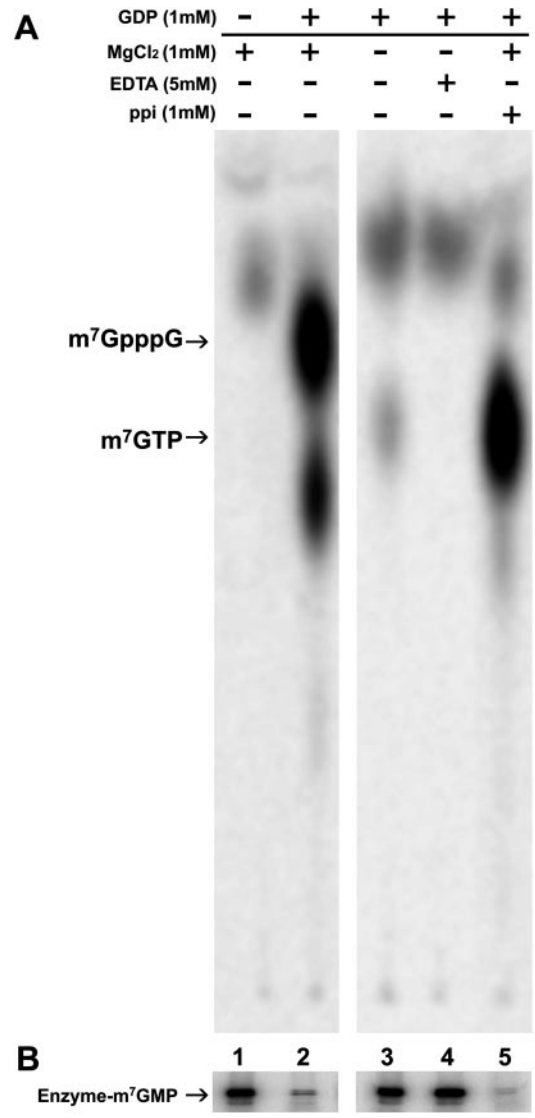

FIG. 5. **Effect of Mg^{2+} and pyrophosphate on the formation of m^{7}GpppG.** The ^{32}P-labeled covalent [Enzyme-m^{7}GMP] intermediate and GDP (1 mM) were incubated at 30 °C for 2 h in buffer conditions as described under "Experimental Procedures" with some modifications as indicated. *Panel A*, half of the reaction mixture was analyzed by TLC. *Arrows* indicate the migration positions of standard m^{7}GpppG and m^{7}GTP. *Panel B*, the other half was analyzed by SDS-PAGE. *Lane 1* is a control without adding GDP in the reaction.

Transfer of m^{7}GMP from the Covalent [Enzyme-m^{7}GMP] Intermediate to Nucleotides—To characterize the reaction after the formation of the covalent [Enzyme-m^{7}GMP] intermediate, the radiolabeled intermediate was purified from the reaction mixture of the capping enzyme, [α-^{32}P]GTP, and AdoMet by metal affinity chromatography (data not shown). Another set of experiments indicated, surprisingly, that a trace of GDP in the preparation of GTP may decrease the accumulation of the covalent intermediate, prompting us to ask whether certain nucleotides could act as acceptors to receive m^{7}GMP from the covalent intermediate. A variety of nucleotides were, therefore, incubated with the purified covalent [Enzyme-m^{7}GMP] intermediate in this study (Fig. 4, *A* and *B*). GDP indeed reduced the amount of the covalent intermediate and produced m^{7}GpppG simultaneously (*lane 2*), suggesting that m^{7}GMP was transferred from the covalent intermediate to GDP rather than being released into the reaction solution in which free m^{7}GMP would have otherwise appeared. ADP also reduced to a lesser extent the amount of the covalent intermediate and produced

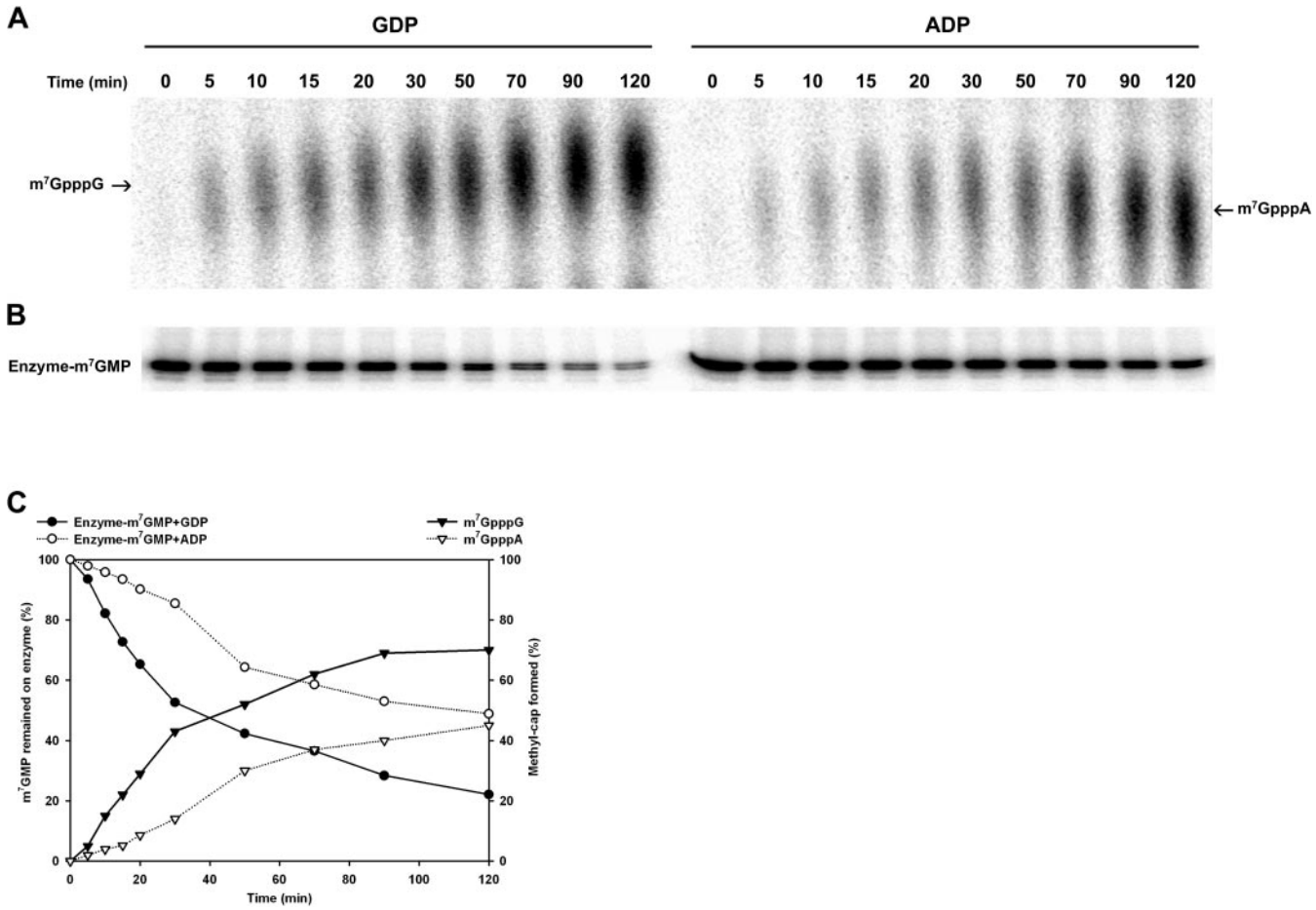

FIG. 6. **Formation rates of m^7GpppG and m^7GpppA.** GDP or ADP (each 1 mM) was incubated with the ^{32}P-labeled covalent [Enzyme-m^7GMP] intermediate at 30 °C for the indicated periods of time in buffer conditions as described under "Experimental Procedures." *Panel A*, TLC analysis shows the accumulation of m^7GpppG and m^7GpppA along the incubation. *Panel B*, SDS-PAGE analysis shows the decrease of the covalent intermediate. *Panel C*, a plot represents the numerical data of pixels of each time point shown on *panel A* and *panel B*. The data of the covalent intermediate at time 0 was referred as 100%.

m^7GpppA (Fig. 4, *A* and *B*, *lane 8*). dGDP and m^7GDP seemed to have limited abilities to receive m^7GMP (*lanes 3* and *4*, respectively). Other nucleotides apparently did not trigger the transfer of m^7GMP onto them. Neither UDP nor CDP could receive m^7GMP from the covalent intermediate (data not shown). Besides m^7GpppG, a minor labeled product with a slow migrating rate also appeared on the TLC plate as m^7GMP was transferred to GDP (Fig. 4*A* and 5*A*, *lane 2*). This product was converted to m^7GpppG after nuclease P1 treatment (Fig. 4*C*, *lane 3*), suggesting that it arose from m^7GMP transfer to an unknown GDP derivative in the GDP preparation. The effects of Mg^{2+} and pyrophosphate on the transguanylation reaction were further examined (Fig. 5). The result of mixing GDP with the covalent intermediate is shown again in *lane 2* as a control. Exclusion of Mg^{2+} from the reaction mixture blocked the transfer reaction (*lanes 3* and *4*), indicating the Mg^{2+}-dependent nature of the reaction. m^7GTP appeared in the reaction products as pyrophosphate was added (*lane 5*), suggesting that the step of forming the covalent [Enzyme-m^7GMP] intermediate (step 3 in the proposed model) is reversible. The rates of transferring m^7GMP from the covalent intermediate to GDP or ADP were compared (Fig. 6). The initial rate of forming m^7GpppG was estimated to be ~2.5-fold faster than that of forming m^7GpppA based on the kinetic data shown on *panel C*.

Transfer of m^7GMP from the Covalent [Enzyme-m^7GMP] Intermediate to RNA—Two RNA molecules, $ppG(C)_{25}$ and $ppA(C)_{25}$, were synthesized *in vitro* and incubated with the radiolabeled covalent intermediate to assay their ability to receive m^7GMP (Fig. 7). The data clearly demonstrated the transfer of m^7GMP from the covalent intermediate to RNA substrates in the period of incubation. The amounts of the covalent intermediate decreased gradually with time, whereas the radiolabeling of RNA increased. The rate of m^7GMP transfer from the covalent intermediate to $ppG(C)_{25}$ was greater than that to $ppA(C)_{25}$ by a factor of ~3.8 according to the kinetic data shown on *panel C*. Taken together with the nucleotide preference described above, we concluded that the BaMV capping enzyme prefers guanylate to adenylate as the acceptor of m^7GMP from the covalent intermediate. RNA molecules with tri, di, or monophosphate at the 5′ end were further assayed in the transfer reactions. Apparently, RNA molecules with a 5′-diphosphate end were ready to receive m^7GMP from the covalent intermediate, whereas molecules with 5′-trisphosphate end were also able to accept m^7GMP albeit to a lesser extent (Fig. 8, *A* and *B*). To examine the cap structures formed at the 5′ end of RNA molecules, the radiolabeled RNA products were recovered, treated with nuclease P1, and analyzed by TLC. Upon the hydrolysis of the reaction products originally from $ppG(C)_{25}$ and $ppA(C)_{25}$, the appearances of m^7GpppG and m^7GpppA were observed, respectively, indicating that normal cap0 structures were formed at the RNA molecules (Fig. 8*C*). m^7GpppG and m^7GpppA instead of $m^7GppppG$ and $m^7GppppA$ were also recovered from products originally from $pppG(C)_{25}$ and $pppA(C)_{25}$, respectively, suggesting that 5′-trisphosphate-terminated RNA was actually not able to receive m^7GMP from the covalent intermediate. The false-positive results shown on

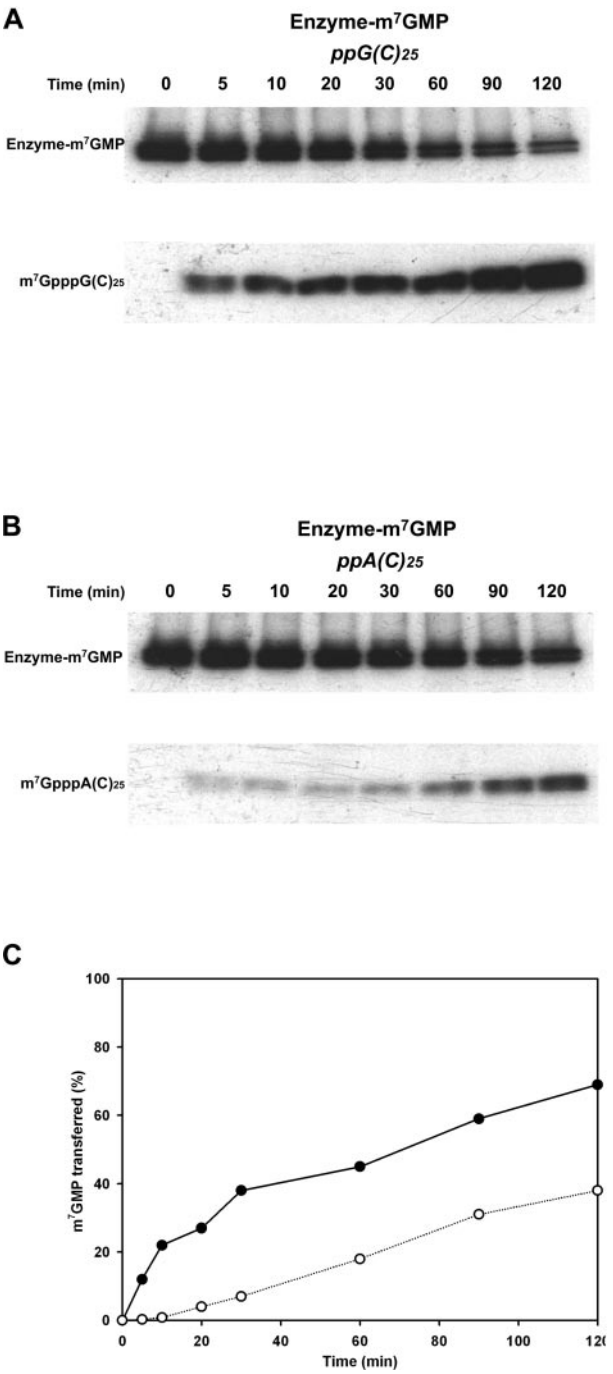

FIG. 7. **Transfer of m^7GMP from the covalent [Enzyme-m^7GMP] intermediate to RNA.** RNA $ppG(C)_{25}$ or $ppA(C)_{25}$ (each 1 μM) was incubated with the ^{32}P-labeled covalent [Enzyme-m^7GMP] intermediate at 30 °C for the indicated periods of time in buffer conditions as described under "Experimental Procedures." SDS (final 2%) was added to stop the reactions, and the products (RNA and protein) were then analyzed by SDS-PAGE (12.5%) and visualized by phosphorimaging. *Panel A*, decreasing of the covalent [Enzyme-m^7GMP] intermediate and concomitant accumulation of $m^7GpppG(C)_{25}$ with time. *Panel B*, decreasing of the covalent intermediate and concomitant accumulation of $m^7GpppA(C)_{25}$. *Panel C*, a plot represents the numerical data of pixel of each time point shown on *panels A* and *B*. The percentage of m^7GMP transfer at time t was estimated as {[pixels of $m^7GpppG/A\text{-}(C)_{25}]_t$/[pixels of $m^7GpppG/A\text{-}(C)_{25}]_t$ + [pixels of [Enzyme-m^7GMP]]$_t$} × 100%. *Lines* in *solid* and *open circles* indicate the transfer of m^7GMP to $ppG(C)_{25}$ and $ppA(C)_{25}$, respectively.

Fig. 8, *panel A* might arise from traces of $ppG(C)_{25}$ and $ppA(C)_{25}$ in $pppG(C)_{25}$ and $pppA(C)_{25}$, respectively, due to the contaminating presence of NDP in the NTP component used in the *in vitro* transcription reaction. In summary, the data thus far conclude that a 5′-diphosphate group at guanosine, adenosine, or RNA is essential for the molecules to accept m^7GMP transferred from the covalent [Enzyme-m^7GMP] intermediate. Because the viral capping enzyme could use RNA as well as nucleotide as the m^7GMP acceptor, knowing the affinities of the two potential acceptors would be important toward understanding the viral replication mechanism. The radiolabeled covalent [Enzyme-m^7GMP] intermediate was, thus, incubated with either $ppG(C)_{25}$ or GDP over a wide range of concentrations. The magnitude of m^7GMP transfer exhibited acceptor concentration-dependent manners with $K_m^{RNA} = \sim 0.4$ μM and $K_m^{GDP} = \sim 0.4$ mM (Fig. 9). The 1000-fold difference in K_m values suggests that RNA is a much more favorable acceptor than mononucleotide to receive m^7GMP from the covalent intermediate.

Transfer of m^7GMP from the Covalent [Enzyme-m^7GMP] Intermediate to BaMV Genomic RNA—Within host cells timely capping of the nascent positive-strand RNA of BaMV should occur to allow the initiation of translation and to prevent RNA from hydrolysis by 5′-exonuclease. It was, therefore, interesting to know when the newly transcribed RNA initiates the process of capping and whether the nucleotide sequences and structures play roles in regulating the process. To answer these questions, RNA molecules with different lengths were synthesized by *in vitro* transcription reactions. RNA 5′-25, 5′-50, 5′-138, and 5′-200 correspond to the first 25, 50, 138, and 200 nucleotides, respectively, of the BaMV genomic RNA. A stem-loop structure encompassing nucleotides 34–118 was predicted using Mfold software (15) (Fig. 10*A*). At first, the 5′-[γ-^{32}P]RNAs were treated with the helicase-like domain of the BaMV replicase to remove the γ-phosphate (Fig. 10*B*) and then incubated with the radiolabeled covalent [Enzyme-m^7GMP] intermediate. The formation of the cap structure at the 5′ end of RNA was indicated by the reappearance of radiolabeling on RNA molecules. The formation of the cap reached a plateau at ~30 min for RNA 5′-138 and 5′-200, whereas RNA 5′-50, and 5′-25 were capped slowly and to lesser extents (Fig. 10*C*). The relative rates of cap formation were compared again by including all the four RNA molecules in a reaction mixture. The cap formation reached a plateau at 30 min for the two longer molecules; nonetheless, the cap formation rates for RNA 5′-50 and 5′-25 were merely ~⅕ and ~1/10, respectively, that for the longer RNA molecules under this competitive condition (Fig. 10, *D* and *E*). To find out the importance of the putative stem-loop structure in the RNA capping process, two RNA molecules were synthesized; one (40–113 rev) has a reverse sequence of nucleotides 44–109 that retains the stem-loop structure, whereas the other (40–113 mut) has sequence altered so that the long stem structure no longer exists (Fig. 11*A*). The two RNA molecules were first treated with the helicase-like domain and then incubated with the radiolabeled covalent [Enzyme-m^7GMP] intermediate. The formation of the cap on RNA 40–113 rev was at a rate ~2-fold faster than that on 40–113 mut (Fig. 11*B*), suggesting that the long stem-loop structure is an important feature for RNA molecules to be capped efficiently.

DISCUSSION

Results in this study allow us to add several details into the proposed working model of the BaMV capping enzyme (1). Upon substrate binding, AdoMet indeed stimulated the cross-linking of GTP to the viral enzyme. An analogous result has been demonstrated in vaccinia virus guanine-N7 methyltransferase in which the cross-linking of the cap structure of RNA to the enzyme is stimulated by concurrent occupancy of the AdoMet/AdoHcy binding site (16). To explain the result, the authors proposed an AdoMet binding-eliciting active-site con-

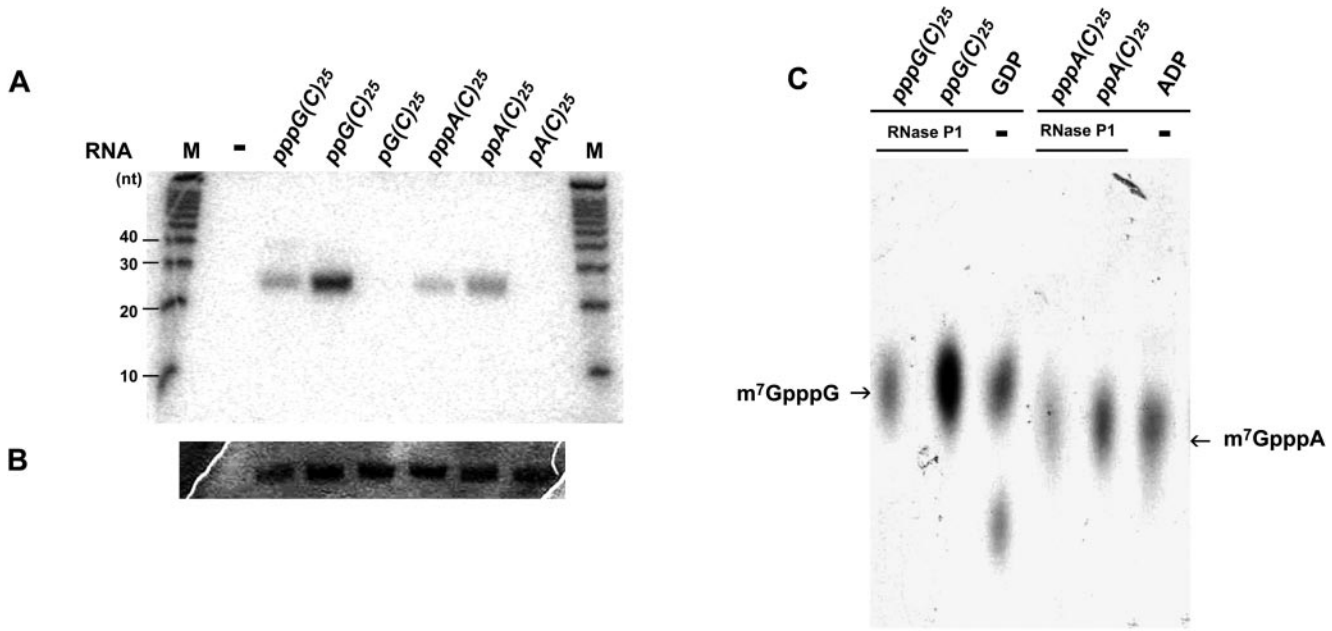

FIG. 8. **Requirement of a diphosphate group at the 5′ end of RNA to accept m^{7}GMP.** RNA substrates with 5′-tri, di, or monophosphates (each 1 μM) were incubated with the ^{32}P-labeled covalent [Enzyme-m^{7}GMP] intermediate at 30 °C for 1 h in buffer conditions as described under "Experimental Procedures." Parts of the reaction mixture were then treated with proteinase K and analyzed by 8 M urea, PAGE (20% polyacrylamide) (*panel A*). *Numbers* on the *left edge* indicate the lengths of RNA markers. *Panel B* shows the presence of RNA by staining the polyacrylamide gel with toluidine blue. RNA molecules in the rest of the reaction mixture were recovered by phenol/chloroform extraction and ethanol precipitation and subsequently treated with RNase P1. The digested products were then analyzed by TLC (*panel C*). *Arrows along* the *edges* of the *plate* indicate the migration positions of markers m^{7}GpppG and m^{7}GpppA. Reactions with GDP or ADP (each 1 mM) as the acceptor for m^{7}GMP transfer were included as controls.

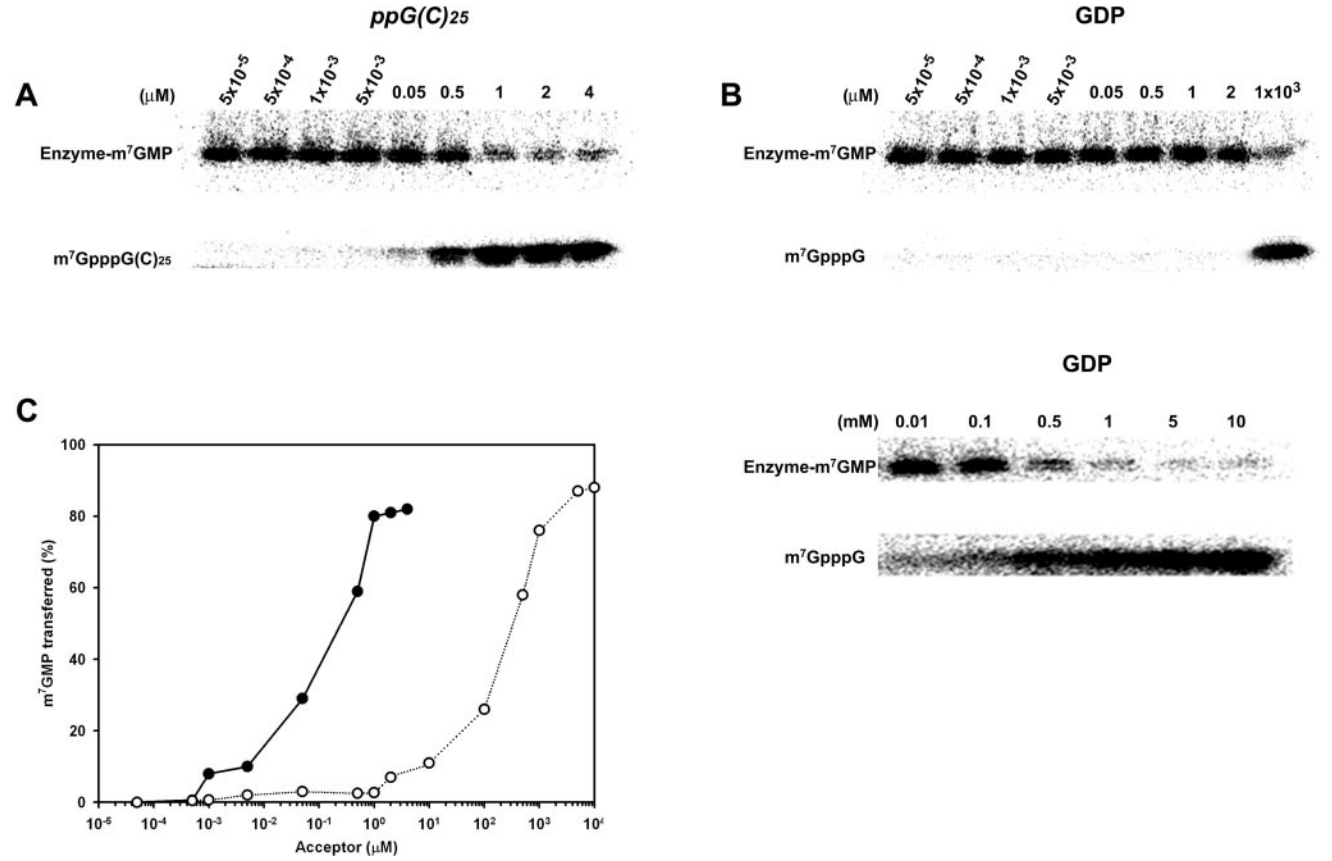

FIG. 9. **Effects of ppG(C)$_{25}$ and GDP concentrations on m^{7}GMP transfer.** ppG(C)$_{25}$ and GDP at various concentrations as indicated were incubated with the ^{32}P-labeled covalent [Enzyme-m^{7}GMP] intermediate at 30 °C for 2 h in buffer conditions as described under "Experimental Procedures." *Panel A*, transfer of m^{7}GMP from the covalent intermediate to ppG(C)$_{25}$. *Panel B*, transfer of m^{7}GMP to GDP. *Panel C*, a plot represents the numerical data of pixels shown on *panel A* and *B*. The transferred percentage of m^{7}GMP at acceptor concentration x was estimated as {[pixels of (acceptor)$_x$]/[pixels of (acceptor)$_x$] + [pixels of [Enzyme-m^{7}GMP]$_x$]} × 100%. *Lines* in *solid* and *open circles* indicate the transfer of m^{7}GMP to ppG(C)$_{25}$ and GDP, respectively.

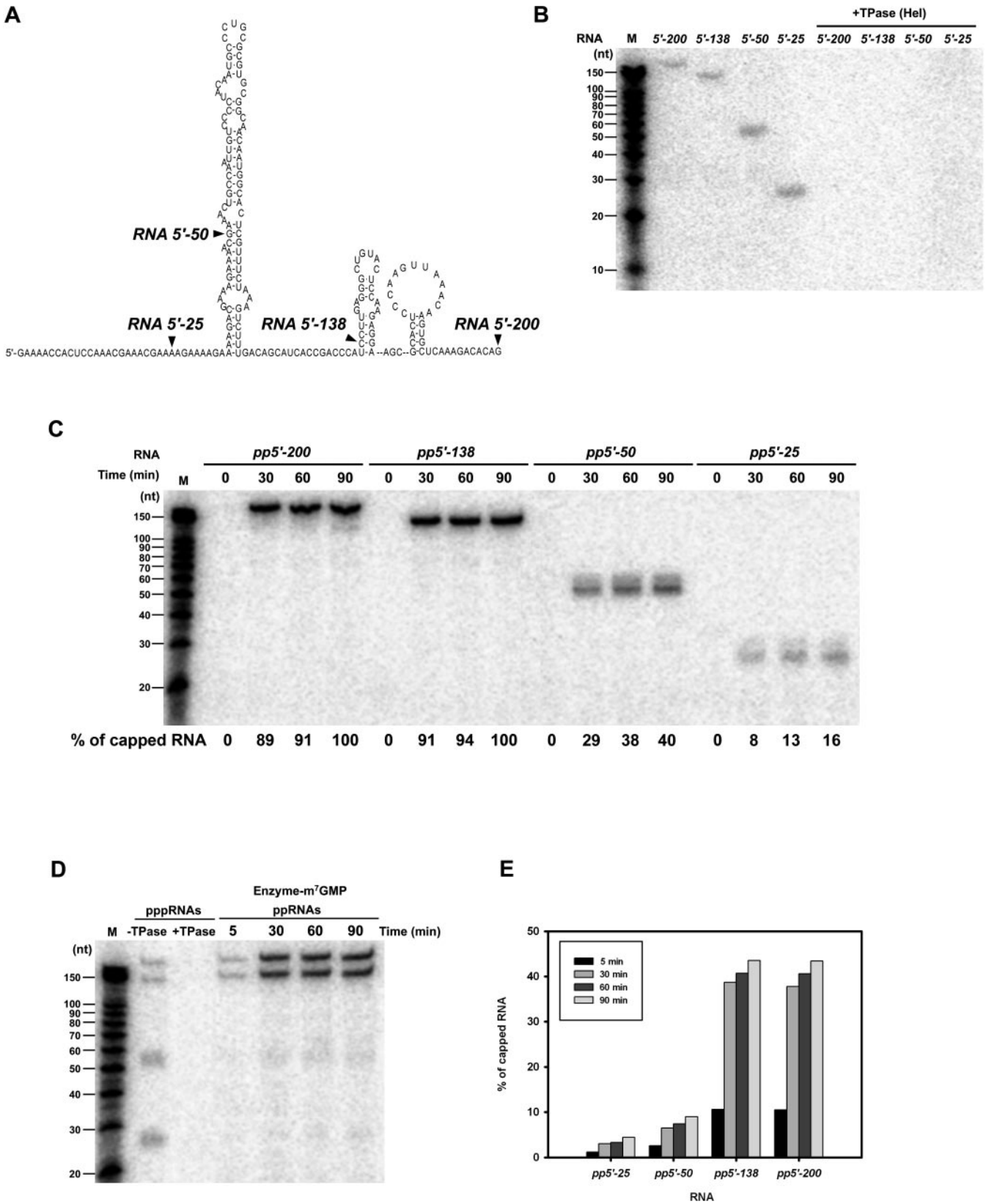

FIG. 10. **Effect of RNA length on the RNA capping efficiency.** *Panel A*, a scheme illustrates nucleotide sequences and Mfold-predicted secondary structures of the RNA molecules. RNA 5′-200, 5′-138, 5′-50, and 5′-25 correspond to the 5′ region of BaMV genome with different lengths indicated by *arrows*. *Panel B*, removal of the 5′ γ-phosphate from the *in vitro* transcribed RNA by 5′-triphosphatase (*TPase*) activity as described under "Experimental Procedures." *Panel C*, 5′-diphosphate RNA (0.06 μM) as indicated was incubated with the ^{32}P-labeled covalent [Enzyme-m^{7}GMP] intermediate at 30 °C for different periods of time in buffer conditions as described under "Experimental Procedures." Proteinase K was added at the ends of reactions, and the RNA products were analyzed by 8 M urea, 12% PAGE and visualized by phosphorimaging. The percentage of capped RNA was estimated by referring the pixels of RNA 5′-200 at 90 min as 100%. *Panels D* and *E*, the four 5′-diphosphate RNA molecules were incubated together with the ^{32}P-labeled covalent intermediates at 30 °C for the indicated periods of time, and the reaction products were analyzed by 8 M urea, 12% PAGE (*panel D*). *M*, M_r markers; *nt*, nucleotides. *Panel E* shows the percentage of capped RNA at every reaction time. The data were estimated by taking the sum of the pixels of RNA molecules at 90 min as 100%.

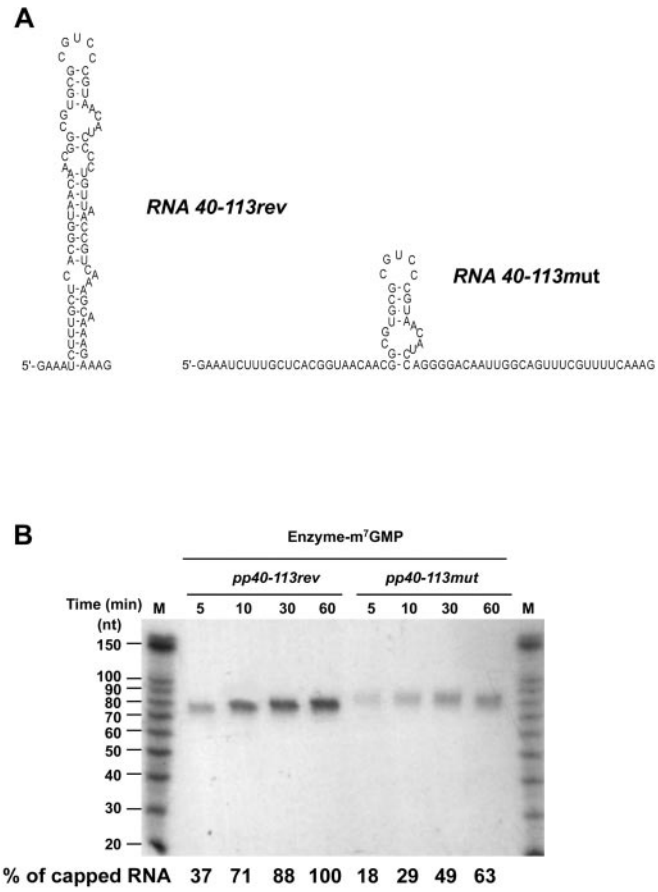

FIG. 11. **Effect of RNA structure on the RNA capping efficiency.** *Panel A*, nucleotide sequences and secondary structures of the RNA molecules predicted by Mfold. RNA 40–113 rev has a reverse sequence of nucleotides 44–109 of the BaMV genome that maintains the stem-loop structure, whereas 40–113 mut has a mutated sequence that abolishes the structure. *Panel B*, RNA 40–113 rev and 40–113 mut were first treated with the helicase-like domain of the BaMV replicase to remove their 5′ γ-phosphate and then incubated with the ^{32}P-labeled covalent intermediate at 30 °C for the indicated periods of time. The percentage of capped RNA was estimated by designating the pixels of RNA 40–113 rev at 60 min as 100%.

formational change, that either (i) enhances the affinity for the cap guanosine at the cap binding site or (ii) alters the protein interface so that a photoreactive moiety is brought closer to the cap structure at the cap site, and as a result, the cap is better poised to be UV-cross-linked to the enzyme. A similar proposition should be applicable to the BaMV capping enzyme (2). Methylation of GTP occurred probably at a much faster rate than the subsequent transfer of m^{7}GMP from m^{7}GTP to an unidentified active-site residue (3). Mg^{2+} was essential for the transguanylation reaction; in contrast, it was dispensable for the transfer of the methyl group from AdoMet to GTP (data not shown) (4). The step of forming the covalent [Enzyme-m^{7}GMP] intermediate is reversible; pyrophosphate could not only exert a product inhibition effect on the forward reaction but also trigger the backward reaction, leading to the regeneration of m^{7}GTP (5). Regarding the structural requirement for acceptors to receive m^{7}GMP from the covalent intermediate, guanylate or adenylate with a 5′-diphosphate group is essential. This property would assure the formation of normal cap structures at the 5′ end of the viral RNA transcripts. Furthermore, there would be no cap at the negative-strand viral RNA, because it is synthesized initially with an uridylate residue (6, 17). In terms of acceptor selectivity, the viral enzyme preferred guanylate to adenylate. A putative stem-loop structure at the 5′ region of the genomic RNA is important for efficient capping reaction of the RNA itself.

The Mg^{2+} dependence and the reversibility of the reaction for the formation of the covalent [enzyme-m^{7}GMP] intermediate probably reflect the chemical natures of the reaction, because similar characteristics have also been demonstrated in reactions of the guanylyltransferase from mammals (18), yeast (19), and vaccinia virus (20). This study also demonstrated that the BaMV capping enzyme can recognize GDP or ADP as an acceptor to receive m^{7}GMP from the covalent intermediate and consequently forms the free cap analog, m^{7}GpppG or m^{7}GpppA, respectively. This property distinguishes the BaMV capping enzyme from that of yeast (19) and mammalian cells (21) in that they cannot cap a mononucleotide. The ~0.4 mM K_m^{GDP} value suggests that m^{7}GpppG has a great chance to exist in the proximity of the viral replication complex within the host cells after all GDP can be provided from the hydrolysis of GTP by the helicase-like domain of the viral replicase (11). This consideration raised the question as to whether m^{7}GpppG, if it does exist, can be the first nucleotide leading the synthesis of the viral RNA transcripts. To answer the question, we have mixed m^{7}GpppG with NTPs in the reaction mixture of the *in vitro* RNA-dependent RNA polymerase assay and found that the addition of m^{7}GpppG actually reduced the synthesis of the positive-strand viral RNA (data not shown), suggesting that pretranscriptional capping is an unlikely event.

This study also showed that GDP is preferred by the covalent [Enzyme-m^{7}GMP] intermediate to donate m^{7}GMP over ADP. This preference was observed also when RNA was the acceptor. This suggests that GDP and ADP should occupy an identical catalytic pocket as their counterparts at the 5′ end of the RNA acceptors during transguanylation; however, the pocket should be spacious enough to accommodate the rest of the RNA substrate. The small K_m value of the RNA acceptor (~0.4 μM for ppG(C)$_{25}$) suggests that the whole part of the RNA substrate contributes to the binding. The genomic RNA of BaMV has a guanylate residue at its 5′ end, whereas the ~2- and ~1-kilobase subgenomic RNAs start with adenylate (22). It is, therefore, interesting to know whether the capping efficiency of the viral RNA would actually be affected by the type of nucleotide at its very 5′ end and whether the speculative difference in the capping efficiency is involved in mechanisms of regulating the viral protein expression. Some viruses of the *Alphavirus*-like superfamily, *e.g.* Semliki Forest virus (23) and Sindbis virus (24), have adenylate at the 5′ end of their genomic RNAs. Do their capping enzymes, in contrast, prefer adenylate to guanylate as the acceptor for m^{7}GMP? Could this be part of the underlying reason for the difference of the first nucleotide in different viruses within the superfamily? Answers for these questions will be valuable toward understanding the role of RNA capping process in the evolution of the viruses.

Timing of the cap formation at the 5′ end of the newly transcribed RNA may be crucial for the survival of virus. A recent study on the capping of human immunodeficiency virus mRNA shows that the capping reaction cannot occur until the nascent mRNA has attained a chain length of 19–22 nucleotides (25). Regarding the genomic RNA of BaMV, we hypothesize that the cap structure is rarely formed before the first 50 nucleotides being synthesized but is formed mostly after the chain of nucleotides is long enough to form the putative stem-loop structure, which may enhance the RNA recognition by the BaMV capping enzyme. Together with the specific interaction of the C-terminal RNA-dependent RNA polymerase domain with the 3′-pseudoknot RNA structure (13), both ends of the genomic RNA may, therefore, interact indirectly with each other via binding of the viral replicase and form a closed loop structure, reminiscent of eukaryotic messenger ribonucleoprotein particle (26). Such a structure would have roles in promot-

ing translation and protecting the viral RNA from degradation. In summary, the dependence of capping efficiency on RNA structure implies that the capping process may participate in regulating the BaMV gene expression. Whether the 5′ regions of the subgenomic RNAs form specific structures and influence the efficiency of capping of their RNA remains to be investigated.

REFERENCES

1. Shuman, S. (1995) *Prog. Nucleic Acid Res. Mol. Biol.* **50,** 101–129
2. Ahola, T., and Kääriäinen, L. (1995) *Proc. Natl. Acad. Sci. U. S. A.* **92,** 507–511
3. Magden, J., Takeda, N., Li, T., Auvinen, P., Ahola, T., Miyamura, T., Merits, A., and Kääriäinen, L. (2001) *J. Virol.* **75,** 6249–6255
4. Merits, A., Kettunen, R., Makinen, K., Lampio, A., Auvinen, P., Kääriäinen, L., and Ahola, T. (1999) *FEBS Lett.* **455,** 45–48
5. Ahola, T., and Ahlquist, P. (1999) *J. Virol.* **73,** 10061–10069
6. Kong, F., Sivakumaran, K., and Kao, C. (1999) *Virology* **259,** 200–210
7. Li, Y.-I., Chen, Y.-J., Hsu, Y.-H., and Meng, M. (2001) *J. Virol.* **75,** 782–788
8. Ahola, T., Laakkonen, P., Vihinen, H., and Kääriäinen, L. (1997) *J. Virol.* **71,** 392–397
9. Huang, Y.-L., Han, Y.-T., Chang, Y.-T., Hsu, Y.-H., and Meng, M. (2004) *J. Virol.* **78,** 1271–1280
10. Lin, N.-S., Lin, B.-Y., Lo, N.-W., Hu, C.-C., Chow, T.-Y., and Hsu, Y.-H. (1994) *J. Gen. Virol.* **75,** 2513–2518
11. Li, Y.-I., Shih, T.-W., Hsu, Y.-H., Han, Y.-T., Huang, Y.-L., and Meng, M. (2001) *J. Virol.* **75,** 12114–12120
12. Li, Y.-I., Cheng, Y.-M., Huang, Y.-L., Tsai, C.-H., Hsu, Y.-H., and Meng, M. (1998) *J. Virol.* **72,** 10093–10099
13. Huang, C.-Y., Huang, Y.-L., Meng, M., Hsu, Y.-H., and Tsai, C.-H. (2001) *J. Virol.* **75,** 2818–2824
14. Huang, F., Bugg, C. W., and Yarus, M. (2000) *Biochemistry* **39,** 15548–15555
15. Zuker, M. (2003) *Nucleic Acids Res.* **31,** 3406–3415
16. Mao, X., and Shuman S. (1996) *Biochemistry* **35,** 6900–6910
17. Cheng, J.-H., Peng, C.-W., Hsu, Y.-H., and Tsai, C.-H. (2002) *J. Virol.* **76,** 6114–6120
18. Venkatesan, S., and Moss, B. (1982) *Proc. Natl. Acad. Sci. U. S. A.* **79,** 340–344
19. Itoh, N., Mizumoto, K., and Kaziro, Y. (1984) *J. Biol. Chem.* **259,** 13930–13936
20. Shuman, S., and Hurwitz, J. (1981) *Proc. Natl. Acad. Sci. U. S. A.* **78,** 187–191
21. Venkatesan, S., and Moss, B. (1980) *J. Biol. Chem.* **255,** 2835–2842
22. Lee, Y.-S., Lin, B.-Y., Hsu, Y.-H., Chang, B.-Y., and Lin, N.-S. (1998) *J. Gen. Virol.* **79,** 1825–1832
23. Takkinen, K. (1986) *Nucleic Acids Res.* **14,** 5667–5682
24. Strauss, E. G., Rice, C. M., and Strauss, J. H. (1984) *Virology* **133,** 92–110
25. Chiu, Y.-L., Ho, C. K., Saha, N., Schwer, B., Shuman, S., and Rana, T. M. (2002) *Mol. Cell* **10,** 585–597
26. Wells, S. E., Hillner, P. E., Vale, R. D., and Sachs, A. B. (1998) *Mol. Cell* **2,** 135–140